

Supplementary information

Multi-Stimuli-Responsive Polymers Enabled by Bio-Inspired Dynamic Equilibria of Flavylum Chemistry

*Yuxi Liu,^{ac} Rico F. Tabor,^a Piotr Pawliszak,^{bc} David A. Beattie,^{bc} Marta Krasowska,^{bc} Benjamin W. Muir,^d San H. Thang^{ac} and Chris Ritchie^{*ac}*

^a School of Chemistry, Monash University, Clayton, VIC 3800, Australia

^b Future Industries Institute, University of South Australia, Mawson Lakes, SA 5095, Australia

^c ARC Centre of Excellence for Enabling Eco-Efficient Beneficiation of Minerals, Australia

^d CSIRO Manufacturing, Bag 10, Clayton South, VIC 3169, Australia.

The supplementary information contains:

1. Materials
2. Instruments and methods
3. Synthesis and composition optimisation of parent polymer (Table S1, S2, Fig. S1) and synthesis of flavylum-containing polymers via post-modification
4. Supplementary thermodynamic UV-vis absorption spectra (Fig. S2)
5. Supplementary schemes of flavylum equilibria network (Scheme S1, S2)
6. Supplementary excitation spectra of flavylum-containing polymers (Fig. S3, S4)
7. Supplementary results for light-responsiveness (Fig. S5)
8. Supplementary results for thermo-responsiveness (Fig. S6)
9. Supplementary ¹H NMR spectra of flavylum-containing polymers (Fig. S7, S8)
10. Supplementary profile analysis tensiometry results and determination of critical aggregation concentration (Fig. S9-12)
11. Supplementary SAXS results (Fig. S13-15, Table S3-5)
12. Supplementary TEM images of flavylum-containing polymers (Fig. S16)
13. References

1. Materials

2,2'-Azobis(isobutyronitrile) (12 wt % in acetone, AIBN) initiator was purchased from Sigma-Aldrich, the acetone removed in vacuo, and the solid recrystallised from methanol before use. *N*-Isopropylmethacrylamide (97% NIPMAM, Sigma-Aldrich), methacryloyl chloride (97%, Sigma-Aldrich), trifluoroacetic acid (99%, Sigma-Aldrich), triethylamine (99%, Sigma-Aldrich), 4-diethylamino salicylaldehyde (98%, Combi-Blocks), 2-hydroxy-4-methoxybenzaldehyde (98%, Sigma-Aldrich); 4-aminoacetophenone (98%, Aarron Chemicals), sulfuric acid (98%, Thermo Fisher Scientific), acetic acid (glacial, Thermo Fisher Scientific), and 4-cyano-4-[(dodecylsulfanylthiocarbonyl)sulfanyl]pentanoic acid (95%, CDTPA, Boron Molecular) were purchased from mentioned sources and used as received. All solvents were analytical or high-performance liquid chromatography (HPLC) grade purchased from commercial sources and used as received. Universal buffer preparation¹: 2.3 cm³ of 85% (w/w) phosphoric acid (Millipore), 7.00 g of citric acid monohydrate (GR, Sigma-Aldrich), and 3.54 g of boric acid (99.5%, Sigma-Aldrich) were dissolved in water; 343 mL of 1 M NaOH aqueous solution was added, and the solution diluted to 1 dm³ with water. pH values were adjusted by the addition of a 1 M NaOH aqueous solution and a 1 M HCl aqueous solution and measured with a pH/ORP/ISE Meter-IC-HI98191 from Hanna Instruments.

2. Instruments and methods

2.1 Profile analysis tensiometry with emerging bubble geometry

The surface tension of polymer solutions was measured by profile analysis tensiometry with emerging bubble geometry (PAT-1M, Sinterface). An air bubble of a constant volume was generated at the end of a U-shape stainless steel needle of 1.998 mm diameter in a quartz cuvette (25mL) containing the polymer solutions at the desired concentrations. The temperature was kept constant at 25.0 ± 0.2 °C using an external computer-controlled heating–cooling circulating bath (300F, Julabo). Two independent repeats were carried out for each concentration. The surface tension was recorded as a function of time until the surface tension reached equilibrium.

2.2 Dynamic light scattering and zeta potential

The particle size distribution and polydispersity index (PDI) of aggregates were determined from correlograms using Zetasizer 8.02 software and measured with a Malvern Zetasizer NANO ZS (Malvern Panalytical, United Kingdom). This instrument was equipped with a 4 mW He–Ne laser source (633 nm) and a backscatter detector set at a 173° angle. Zeta potential was determined on the same device through electrophoretic mobility measurements using a closed capillary electrophoresis cell (DTS1070, Malvern Panalytical, United Kingdom). All experiments were conducted at 25 °C in triplicate.

2.3 Small angle X-ray scattering

SAXS experiments were performed at the SAXS/WAXS beamline at the Australian Synchrotron, ANSTO using an autoloader². X-ray scattering (photon energy = 15.0 keV, wavelength $\lambda = 0.827$ Å) was measured using a Pilatus3 2M detector (Dectris, Switzerland). Two-dimensional (2D) scattering images were recorded over a q -range from 0.00194 – 0.203 Å⁻¹. A silver behenate standard was used to calibrate the sample-to-detector distance (7000 mm.) The 2D scattering images recorded were converted to 1D scattering profiles of scattered X-ray intensity $I(q)$ versus q by radial averaging using Scatterbrain version 2.82 software. The data from the detector configuration were background subtracted in Scatterbrain (v2.82) and form-factor modelling was performed using SasView (version v5.0.6).

2.4 Transmission electron microscopy

Transmission electron microscopy (TEM) was performed on a FEI Tecnai Spirit G2 TEM. The samples were prepared by dropping the solutions over a copper grid, which was glow discharged at 30 mA for 30 s using a Pelco easiGlow instrument. The samples were negatively stained by uranyl acetate (2 wt%) to increase the contrast.

2.5 Cryogenic electron microscopy

Quantifoil R1.2/1.3 200 mesh copper grids or Lacey carbon-supported copper grids were glow discharged at 30 mA for 30 s using a Pelco easiGlow instrument. Polymer solutions (10 g/L) were applied to grids and rapidly vitrified in liquid ethane. The vitrification process was performed using the Thermo Fisher Scientific Vitrobot Mark IV system with a blot force of 4 for 3.5 seconds. The temperature was maintained at 4 °C with 100% relative humidity. Then the data collection was carried out on a FEI Tecnai Spirit G2 TEM using a Gatan 626 Cryo transfer holder. The nominal defocus range was set between -1.0 and -2.0 μm.

2.6 Nuclear magnetic resonance spectroscopy (NMR)

^1H NMR spectra were recorded on a Bruker Avance 400 NMR spectrometer at frequencies of 400 MHz NMR, chemical shifts (δ) are reported in ppm and were calibrated against residual solvent signals of $\text{D}_2\text{O}-d_2$ (δ 4.79) and $\text{MeOD}-d_4$ (δ 3.31). Samples were dissolved in $\text{D}_2\text{O}-d_2$ and $\text{MeOD}-d_4$ at 5-10 mg mL $^{-1}$. The data are reported as chemical shift (δ).

2.7 Stock solution preparation

$\text{Et}_2\text{N-FlavP}_1$ and MeO-FlavP_1 were dissolved in deionised water to make a stock solution (10 g/L), after sonication for 15 min, the stock solution was kept in the fridge at 4 °C for 30 min before any further dilution. The freshly prepared stock solution was diluted to 0.1 g/L in universal buffer solutions at the desired pH and kept in the dark for 24 hours for equilibration before any tests were conducted on UV-vis spectroscopy and photoluminescence spectroscopy.

2.8 UV-visible absorption/transmittance spectroscopy

Absorption and transmittance spectra were collected on an Agilent technologies Cary 60 UV-vis spectrophotometer using Agilent Technologies standard quartz cuvettes of 1 or 0.1 cm path length. Baseline corrections were applied over the entire collected wavelength range for each solvent.

2.8.1 Thermodynamics by UV-vis absorption spectroscopy

The 24-hour thermodynamic data were recorded at varying intervals: 0–0.5 hours (2-minute intervals), 0.5–2 hours (5-minute intervals), and 2–24 hours (30-minute intervals).

2.8.2 pH-dependent chromism by UV-vis absorption spectroscopy

The stock solutions were diluted into universal buffers (pH 1 to 12) and incubated in the dark at room temperature for 24 hours before the UV-vis spectroscopy measurements. In universal buffers, mild precipitation of the polymers was expected after being left undisturbed due to the low absolute value of their zeta potential. When precipitation occurred after the 24-hour equilibration, the solutions were shaken to ensure homogeneity before promptly collecting the spectra. In most cases, the spectra baselines were consistent across samples. However, baseline adjustments ($|\text{adjustment}| < 0.04$ OD) were applied to the following data to align with other spectra: $\text{Et}_2\text{N-FlavP}_1$ at pH 2, 4, 7 (**Fig. 2A** in main text) and MeO-FlavP_1 at pH 1 (**Fig. 2D** in main text).

2.8.3 Photo-responsiveness tests by UV-vis absorption spectroscopy

The wavelengths of the LED lights are 365 nm for MeO-FlavP_1 and 455 nm for $\text{Et}_2\text{N-FlavP}_1$ (2 mL, 0.1 g L $^{-1}$) The input power was controlled and set to 2.1 W by adjusting the voltage and current of the LEDs. The irradiation durations before each spectral collection were 1 min, 1 min, 3 min, 5 min, 10 min and 10min, resulting in accumulated irradiation durations of 1 min, 2min, 5min, 10 min, 20 min and 30min. The photoconversion rate is calculated by dividing the change ($\text{Abs}_{\text{before}} - \text{Abs}_{\text{after}}$) in absorbance by the irradiation time (in seconds). The rate is plotted against the sum of the most recent irradiation time and half the latest irradiation duration. For instance, the second irradiation is plotted at 90 seconds ($60 + 60/2$), and the third at 210 seconds ($120 + 180/2$).

2.8.4 Temperature-responsiveness by UV-vis transmittance spectroscopy

The thermo-responsive properties were evaluated using UV-vis transmittance spectroscopy, by monitoring the change in transmittance ($\lambda = 700 \text{ nm}$) of the polymer aqueous solutions (1 g L^{-1}) collected after 5 minutes of incubation at each temperature.

2.9 Photoluminescence (PL) spectroscopy

Steady-state fluorescence measurements were taken on a Varian Cary Eclipse fluorescence spectrophotometer with a testing voltage of 600 V. The emission spectra were obtained from the equilibrated solutions at each pH by exciting at the wavelength of $\lambda_{\text{exc}} = 530 \text{ nm}$ or 455 nm for Et₂N-FlavP₁, and $\lambda_{\text{exc}} = 465 \text{ nm}$ or 365 nm for MeO-FlavP₁.

2.10 Gel permeation chromatography (GPC)

GPC was performed on a system comprising a Shimadzu LC-20AT pump, a Shimadzu RID-20A refractive index detector, and an SPD-20A UV-visible detector. The GPC is equipped with a guard column (WAT054415) and 3× Waters GPC columns (WAT044238, WAT044226, WAT044235, 300 mm × 7.8 mm). The eluent is DMF with 10 mM LiBr and eluted at 1 mL min^{-1} for 45 min in total. The samples were dissolved in DMF with 10 mM LiBr and filtered through 0.20 μm syringe filters. A calibration curve was obtained from poly(methyl methacrylate) (PMMA) standards (Agilent) ranging from 960 to 1 568 000 g mol^{-1} .

3. Synthesis and composition optimisation of parent polymer and synthesis of flavylum-containing polymers via post-modification

3.1 Synthesis of parent polymer poly(NAPhMA-co-NIPMAM) using a Chemspeed swing

Monomer *N*-(4-acetylphenyl)methacrylamide (NAPhMA) was synthesised according to previous method.⁴ 4-Aminoacetophenone was dissolved in dichloromethane (with triethylamine, 2 times the equivalent to 4-aminoacetophenone). Methacryloyl chloride was added dropwise into the solution in an ice bath and stirred overnight at room temperature. The precursor monomer NAPhMA was purified by recrystallisation in methanol, resulting in colourless crystals (yield 90%).

The parent polymers in our previous work are not water-soluble, to increase the processability of the parent polymers, the idea is to make the parent polymers more water-soluble to synthesise water-soluble flavylum-containing polymers that can be potentially used as surfactants. Thus, both monomers remained the same, the feed ratio was changed to favour a more hydrophilic polymer product. A Chemspeed swing (Chemspeed Technologies Pty Ltd) equipped with an ISYNTH reactor was used at the beginning to optimise the composition of the copolymers.

When the synthesis was initially performed within an ISYNTH unit, the monomer conversions (both <50%) were significantly lower than what could be achieved in the lab when operated on the Schlenk line. This could be due insufficient purging to deoxygenate the solutions. Thus, in the presented trial, the ratio of initiator to RAFT agent is adjusted from 0.2:1 to 0.5:1 for the Chemspeed synthesis.

The synthesis was carried out using the following method. Solutions at the desired concentrations of CDTPA (RAFT agent), ABIN (initiator), NAPhMA (M_1) and NIPMAM (M_2) were prepared in volumetric flasks in DMF. The solutions were then purged with nitrogen for 1 hour before being transferred into the Chemspeed deck which was purged with nitrogen. The solutions were aspirated using the 4-Needle head tool into each glass ISYNTH vial according to the pre-programmed settings to target the desired composition ratio. The ISYNTH reactors were kept under nitrogen at 70 °C with orbital shaking at 400 rpm for 24 hours, after which the reaction was quenched by cooling down the temperature and exposing the reaction to air, a small portion of each solution was taken out for ¹H NMR analysis. The conversions and degree of polymerisation of each polymerisation were summarised in **Table S1**. However, none of the polymer products were water soluble. The dispersity of the polymers was also much higher than a controlled polymerisation: For Entry 1, Dispersity (\mathcal{D})= 1.5 and for Entry 6, Dispersity (\mathcal{D}) = 1.8.

Table S1 Chemspeed synthesis of parent polymer poly(NAPhMA-*co*-NIPMAM)

Entry	Molar ratio in feed [R]:[I]:[M ₁]:[M ₂] ^a	Target DP(M ₁ + M ₂)	conv. M ₁ ^b	conv. M ₂ ^b	DP ^c (M ₁)	DP ^c (M ₂)	M _{n,th} ^d Da	Water Solubility
1	1:0.5:19.9:180.1	200	56.2	47.6	11.2	85.8	13600	insoluble
2	1:0.5:23.4:176.6	200	56.3	48.1	13.2	84.9	13900	insoluble
3	1:0.5:27.1:172.9	200	51.8	48.9	14.0	84.5	14000	insoluble
4	1:0.5:30.8:169.2	200	50.7	47.4	15.6	80.2	13800	insoluble
5	1:0.5:34.5:165.5	200	56.3	50.7	19.4	83.9	15000	insoluble
6	1:0.5:38.4:161.6	200	62.9	53.1	24.1	85.8	16200	insoluble

^a R: RAFT agent, CDTPA; I: initiator, AIBN; M₁: NAPhMA; M₂: NIPMAM. ^b Conversion of the monomers, obtained by crude ¹H NMR. Monomer conversion calculated based on crude ¹H NMR spectra with method from our previous work.⁴ ^c Degree of polymerisation, obtained by crude ¹H NMR. ^d $M_{n,th} = \text{conversion} \times \text{target NAPhMA DP} \times M_w(\text{NAPhMA}) + \text{conversion} \times \text{target NIPMAM DP} \times M_w(\text{NIPMAM}) + M_w(\text{CDTPA})$.

3.2 Synthesis of parent polymer poly(NAPhMA-*co*-NIPMAM)

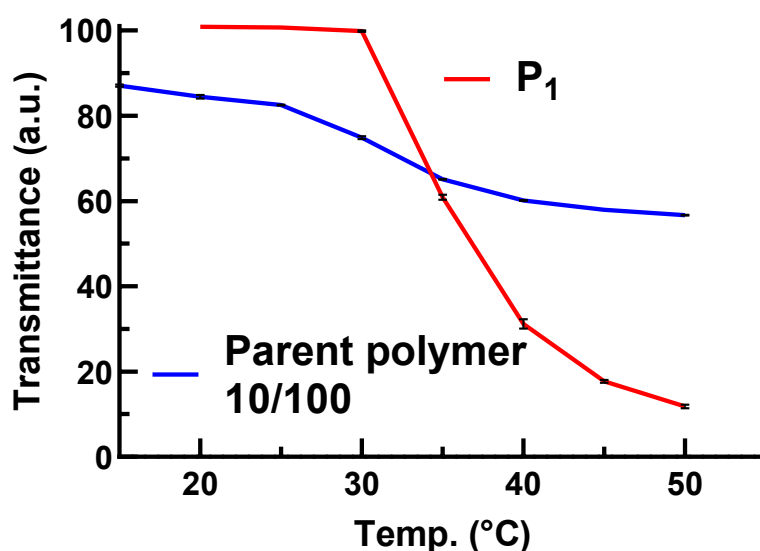
The feed ratio of NIPMAM was therefore increased and the syntheses were transferred on a Schlenk line: the monomers NAPhMA and NIPMAM, RAFT agent CDTPA and initiator AIBN of a desired ratio in feed were dissolved in methanol, degassed on a Schlenk line and the reaction started by heating to 70 °C for 24 hours. A small portion of the solution was sampled to determine conversion using ¹H NMR. The remainder of the solution was precipitated by the addition of cold diethyl ether and redissolved in methanol. It was reprecipitated an additional two times to obtain the random copolymer of NAPhMA and NIPMAM as a pale yellow solid.

The composition of random NAPhMA copolymers is adjusted to tune the water solubility of the parent polymers. The parent polymer with a molar ratio in feed of 10:100 (NAPhMA to NIPMAM) presents a more turbid suspension in water at lower temperatures (**Fig. S1**). When the temperature increases, a sharp transmittance decrease can be observed in this case at 25 °C, which explains that when we were trying to determine the size of the aggregates formed by this parent polymer, at 25 °C the hydrodynamic diameter (D_h) obtained by dynamic light scattering (DLS) were of poor quality as the solution has become too turbid. The parent polymer with a molar ratio in feed of 10:200 (NAPhMA to NIPMAM) was chosen as the candidate of this study (P₁).

Table S2 Characterisations of different parent polymers

Molar ratio in feed	DP (NAPhMA:NIPMAM) ^b	$M_{n, th}$ ^c	$M_{n, GPC}$ ^d	\bar{D} ^d (M_w/M_n)	Water Solubility
[R]:[I]:[M ₁]:[M ₂] ^a					
1:0.2:10:100	8:55	9100	10600	1.37	Cloudy suspension in water at room temperature
1:0.2:10:200	6:88	13000	11800	1.37	Soluble at room temperature

^a R: RAFT agent, CDTPA; I: initiator, AIBN; M₁: NAPhMA; M₂: NIPMAM. ^b Degree of polymerisation, obtained by crude ¹H NMR. ^c $M_{n, th}$ = conversion × target NAPhMA DP × M_w (NAPhMA) + conversion × target NIPMAM DP × M_w (NIPMAM) + M_w (CDTPA). ^d Obtained by gel permeation chromatography (GPC).

**Fig. S1** Cloud point determination of polymers in **Table S2** using UV-vis transmittance spectra.

3.3 Synthesis of flavylium-containing polymers via post-modification

For post-modification, the parent polymer P₁ (200 mg, 23 μ mol) and 1.5 equivalents to the NAPhMA content (136 μ mol) of the 4-diethylamino salicylaldehyde (40 mg, 204 μ mol) or 2-hydroxy-4-methoxybenzaldehyde (31 mg, 204 μ mol) were dissolved in 1.8 mL of acetic acid. Then 0.2 mL of sulphuric acid was added slowly to the solution in an ice bath and the reaction was stirred at room temperature for 72 hours. The solution was first precipitated in cold diethyl ether, redissolved in methanol and reprecipitated in ethyl acetate for three times. The acid in the reaction was not completely removed from the polymer product, which resulted in quite acidic pH both polymers on dissolution in deionised water (1 g L⁻¹): pH 2.4 for Et₂N-FlavP₁ and 2.0 for MeO-FlavP₁.

Supplementary thermodynamic UV-vis absorption spectra

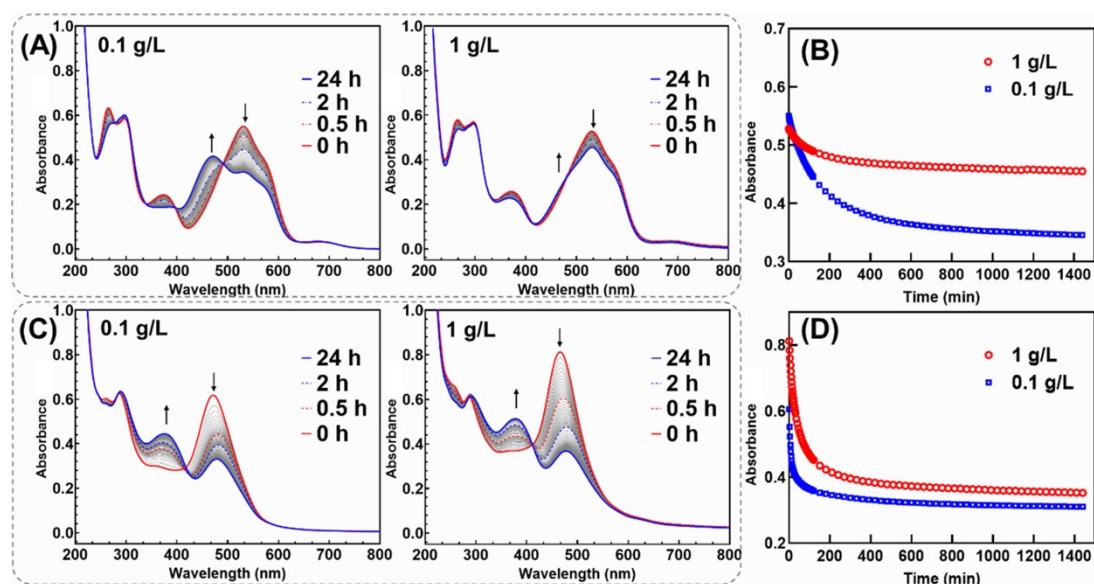
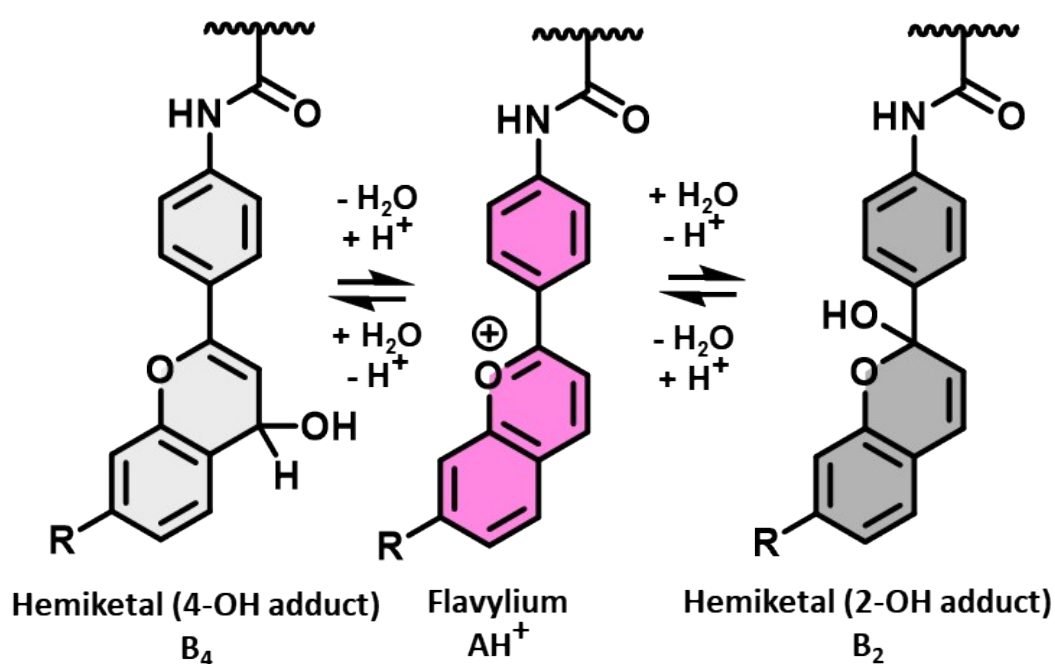


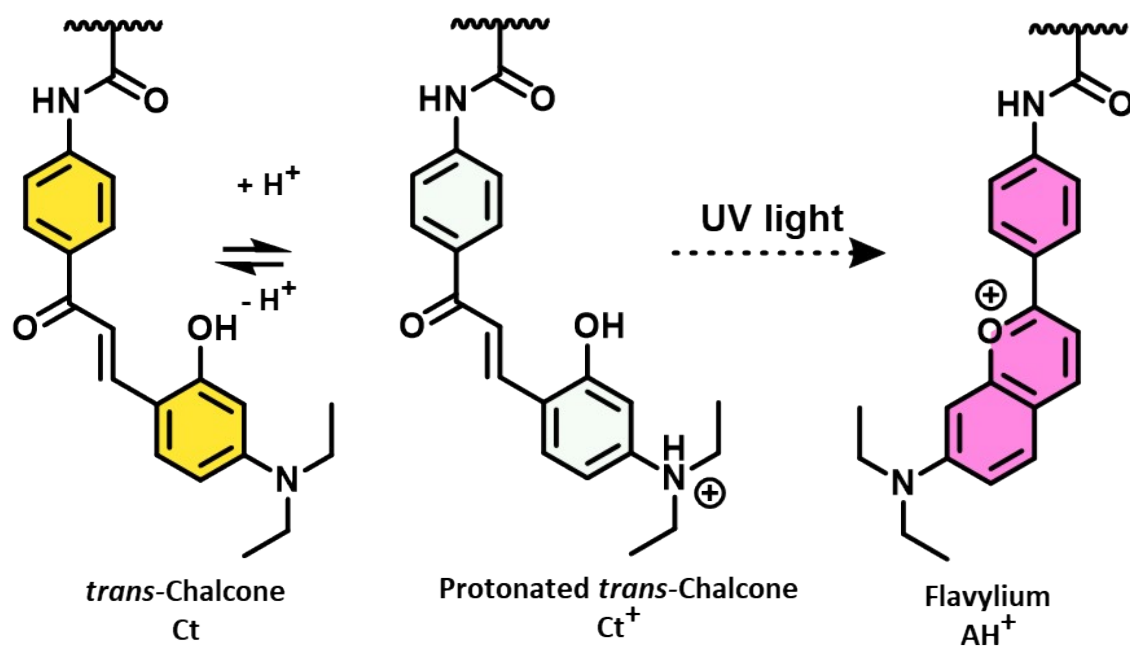
Fig. S3 (A) UV-vis spectra of Et₂N-FlavP₁ at 0.1 g L⁻¹ (pH 3.0) and 1 g L⁻¹ (pH 2.4); (B) a summary of the absorbance at $\lambda = 530$ nm over time in thermodynamic spectra of Et₂N-FlavP₁; (C) UV-vis spectra of MeO-FlavP₁ at 0.1 g L⁻¹ (pH 2.9) and 1 g L⁻¹ (pH 2.0) at 25 °C; (D) a summary of the absorbance at $\lambda = 465$ nm over time in thermodynamic spectra of MeO-FlavP₁.

It is observed that in both cases, the flavylum structures at the higher concentrations of polymers in solutions equilibrated at a higher absorption of the flavylum. This can be rationalised by the increased acidity of the solution on increased concentration due to increased concentration of bisulphate counterions, deprotonations from the flavylum and residual acid in the polymers.

4. Supplementary schemes



Scheme S1 Equilibria of conversion of flavylium in the polymers into two different hemiketal adducts at different positions of the flavylium core.



Scheme S2 Photoconversion of Et₂N-*trans*-chalcone into Et₂N-Flavylium at acidic environment.⁵

5. Supplementary excitation spectra of flavylum-containing polymers

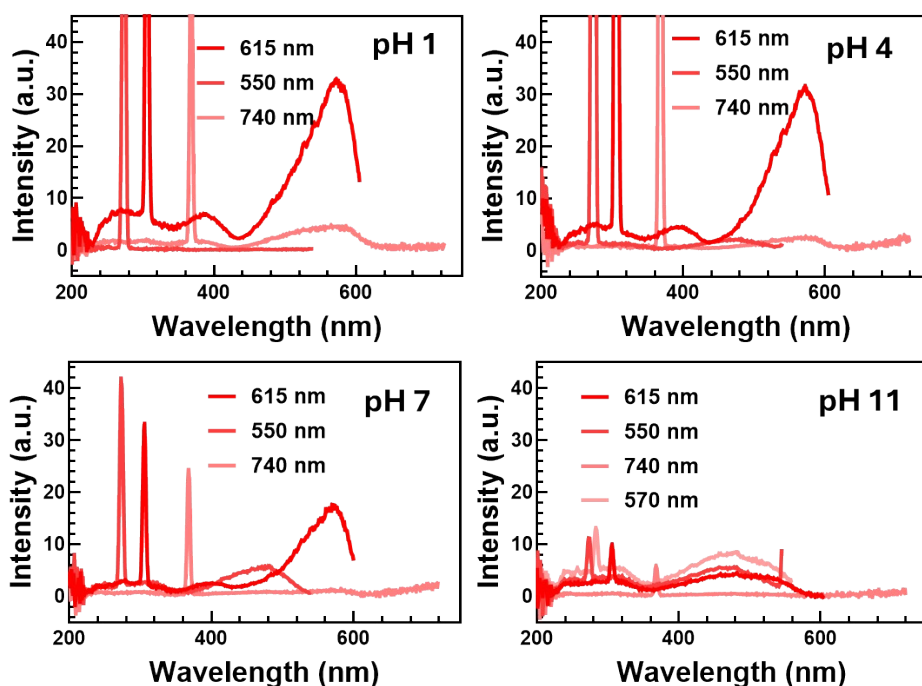


Fig. S4 Excitation spectra ($\lambda_{em}=550$ nm, 615 nm, 740 nm and 570 nm (pH 11 only)) of Et₂N-FlavP₁ (0.1 g L⁻¹) in universal buffers at different pH levels after incubation for 24 hours in the dark. The appearance of chalconate as a species different from others in the equilibrium, for which the excitation spectrum at pH 11 was significantly different compared to other conditions.

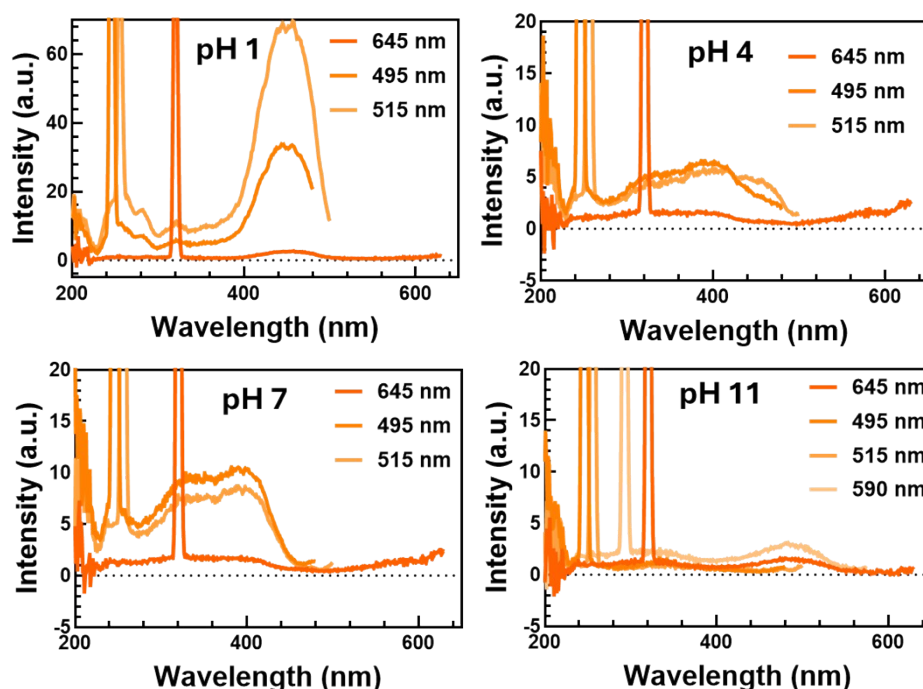


Fig. S5 Excitation spectra ($\lambda_{em}=495$ nm, 515 nm, 645 nm and 590 nm (pH 11 only)) of MeO-FlavP₁ (0.1 g L⁻¹) in universal buffers at different pH levels after incubation for 24 hours in the dark. The appearance of chalconate as a species different from others in the equilibrium, for which the excitation spectrum at pH 11 was significantly different compared to other

conditions.

6. Supplementary results for light-responsiveness

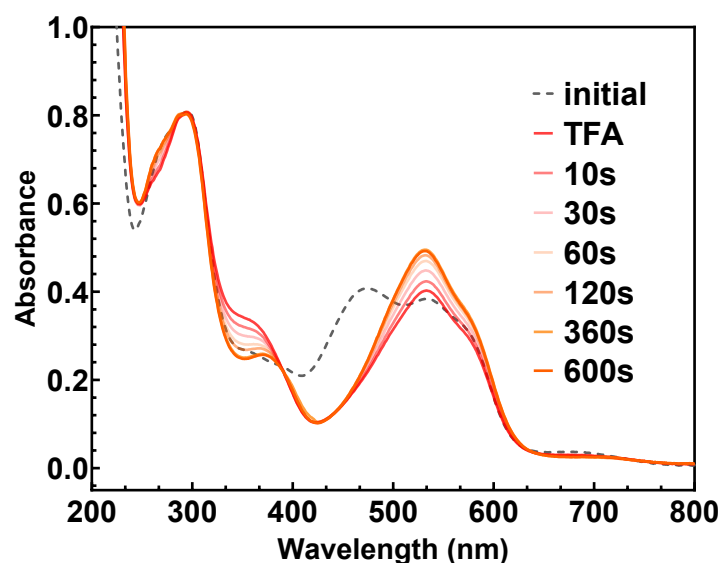


Fig. S5 Et₂N-FlavP₁ (0.1 g L⁻¹ in deionised water, after 24 hours equilibration in the dark and then the irradiation process was conducted). After the irradiation with 455 nm light source, 30 μ L of TFA was added into the solution, the spectra were then collected until a stationary state was achieved at $\lambda = 530$ nm to give the curve with the legend 'TFA'. It is observed that after the addition of TFA, the Ct absorption disappeared, which indicated that protonated chalcone Ct⁺ was generated. Then the solution was irradiated with UV light ($\lambda_{\text{exc}} = 365$ nm) for 10 minutes. The conversion from Ct⁺ to AH⁺ is observed.

7. Supplementary results for thermo-responsiveness

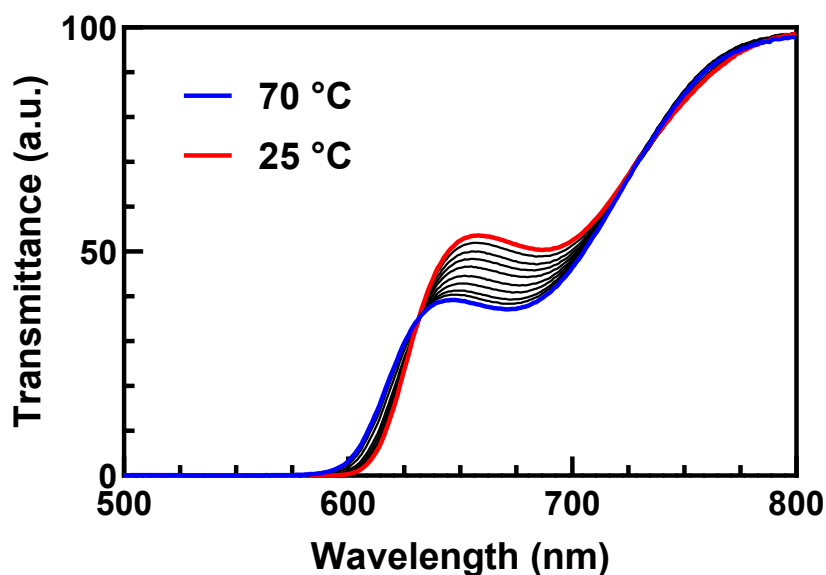


Fig. S6 UV-vis transmittance spectra of Et₂N-FlavP₁ (1 g L⁻¹) with increasing temperature.

8. Supplementary ^1H NMR spectra of flavylum-containing polymers

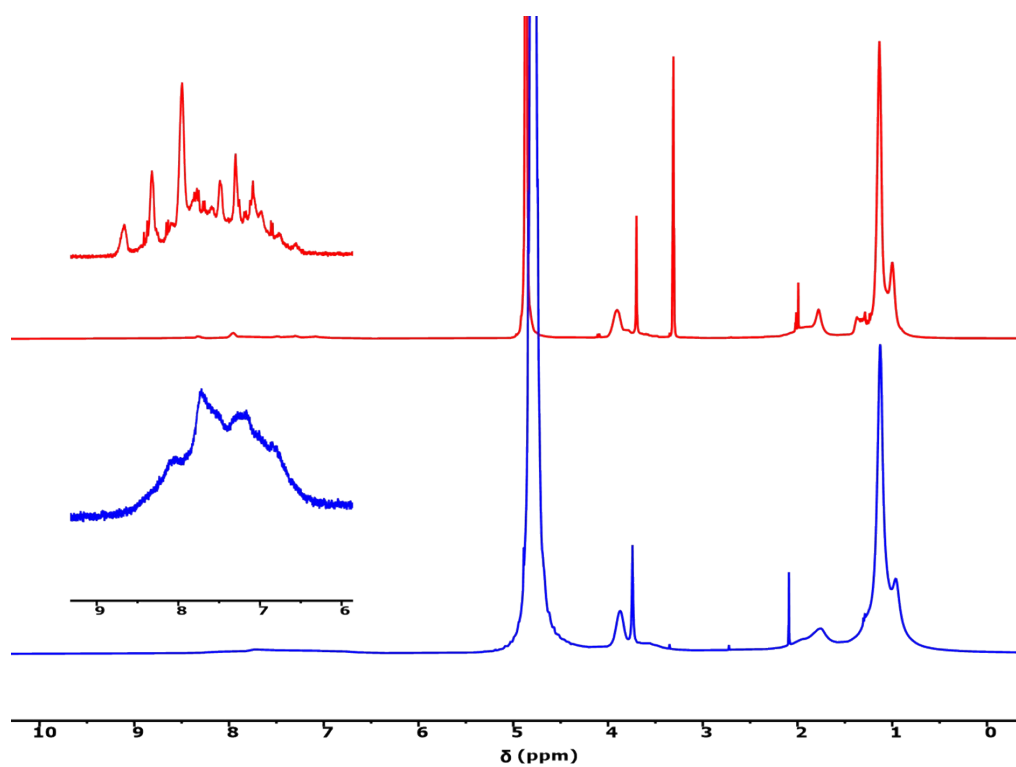


Fig. S7 ^1H NMR spectra (zoomed-in aromatic region) of $\text{Et}_2\text{N-FlavP}_1$ in $\text{MeOD-}d_4$ (red) and $\text{D}_2\text{O-}d_2$ (blue).

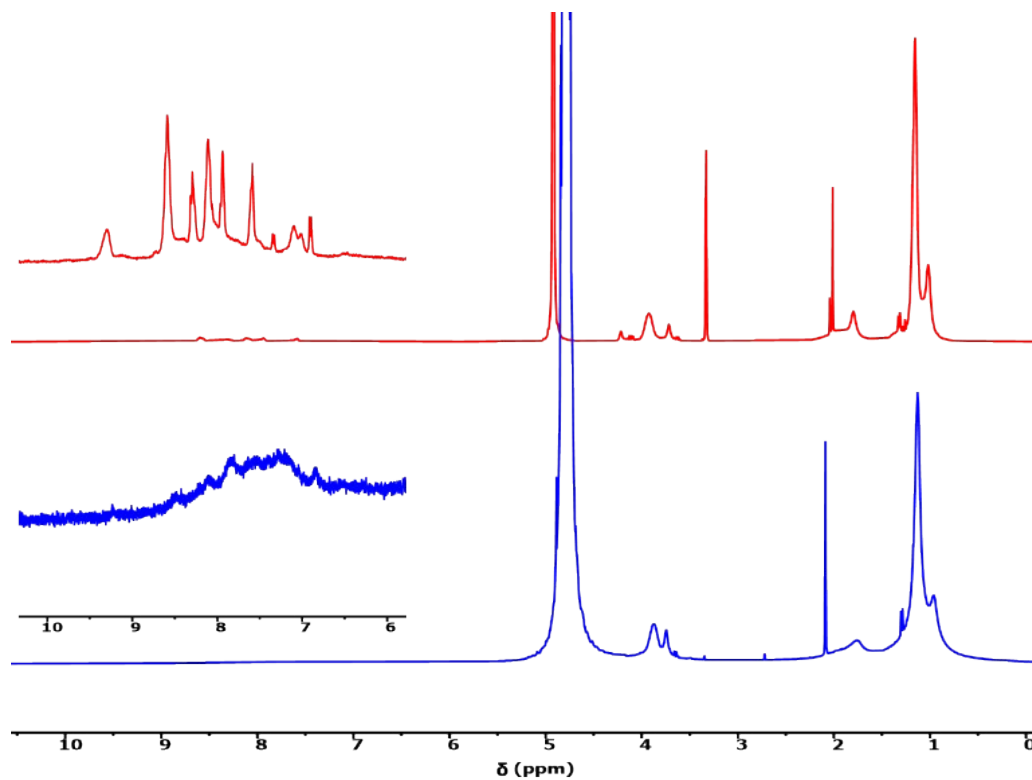


Fig. S8 ^1H NMR spectra (zoomed-in aromatic region) of MeO-FlavP_1 in $\text{MeOD-}d_4$ (red) and $\text{D}_2\text{O-}d_2$ (blue).

9. Supplementary profile analysis tensiometry results and determination of critical aggregation concentration

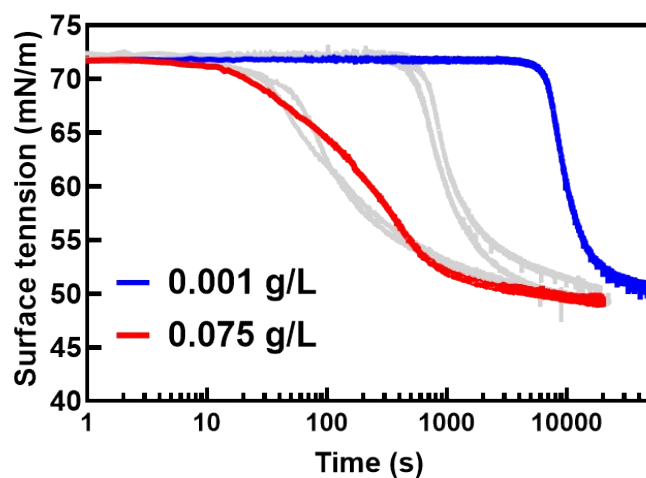


Fig. S9 Surface tension change of $\text{Et}_2\text{N-FlavP}_1$ aqueous solutions as a function of time at different concentrations.

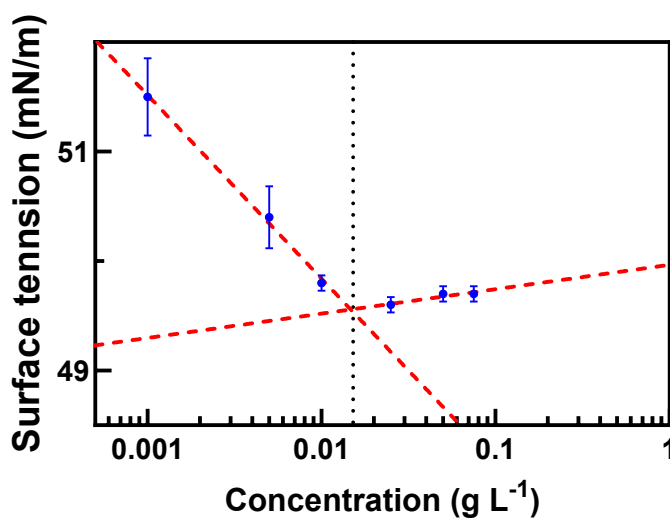


Fig. S10 An illustration of finding the CAC of parent polymer $\text{Et}_2\text{N-FlavP}_1$ by plotting the equilibrium surface tension against concentration.

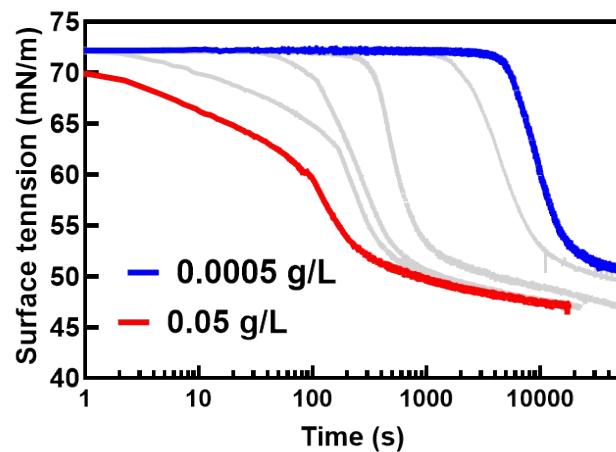


Fig. S11 Surface tension change of MeO-FlavP₁ aqueous solutions as a function of time at different concentrations.

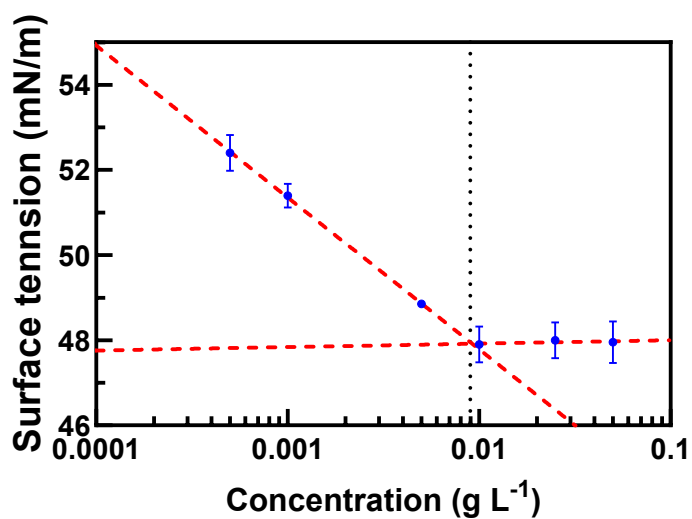


Fig. S12 An illustration of finding the CAC of parent polymer MeO-FlavP₁ by plotting the equilibrium surface tension against concentration.

10. Supplementary SAXS results

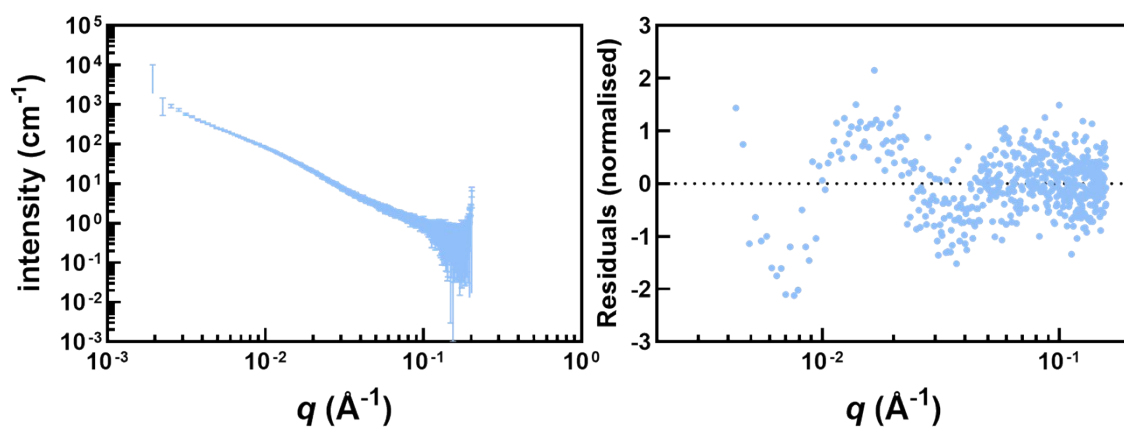


Fig. S13 original SAXS data and fitting residues of P₁.

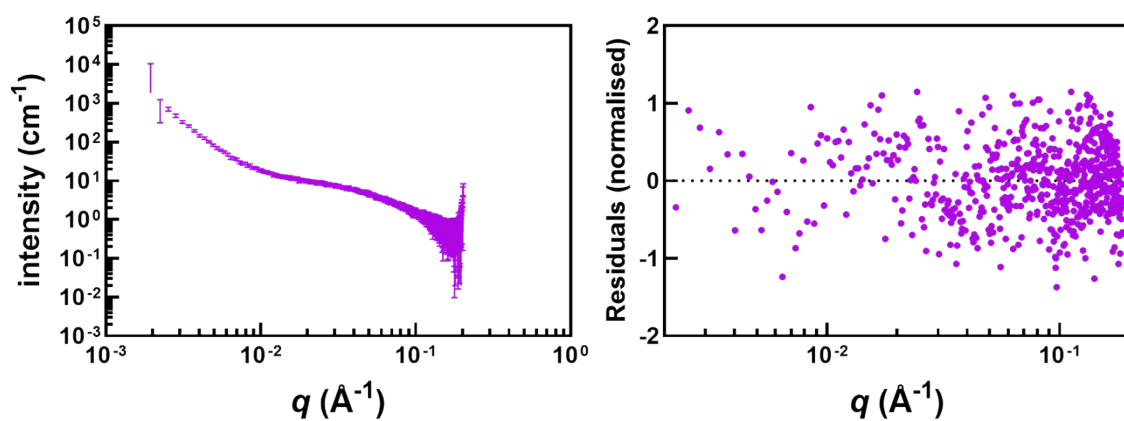


Fig. S14 original SAXS data and fitting residues of Et₂N-FlavP₁.

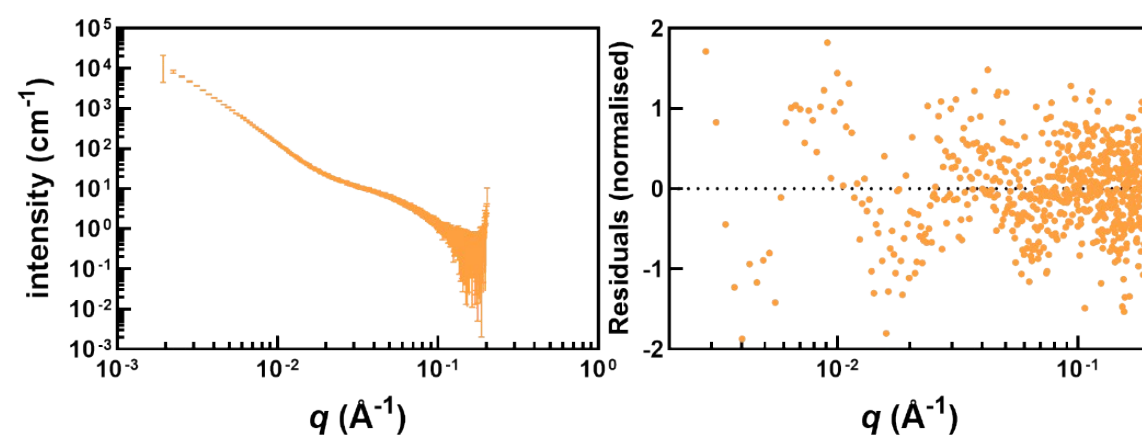


Fig. S15 original SAXS data and fitting residues of MeO-FlavP₁.

Table S3 SAXS Fitting results of P₁ in aqueous solution (10 g L⁻¹)

Polymer	P ₁
Model	Fractal
Scale	0.8730
Background (cm ⁻¹)	0.1726
Volfraction	0.01
Radius (Å)	14.937
Fractal_dim	2.2229
Cor_length (Å)	223.11
Sld_block (10 ⁻⁶ Å ⁻²)	1.9875
Sld_solvent (10 ⁻⁶ Å ⁻²)	9.44
Fitting error χ^2	0.3820

Table S4 SAXS fitting results of Et₂N-FlavP₁ in aqueous solution (10 g L⁻¹)

Polymer	Et ₂ N-FlavP ₁
Model	Fractal core shell
Scale	68.70
Background (cm ⁻¹)	0.5032
Radius (Å)	25.816
Thickness (Å)	46.477
Sld_core (10 ⁻⁶ Å ⁻²)	14.179
Sld_shell (10 ⁻⁶ Å ⁻²)	9.5273
Sld_solvent (10 ⁻⁶ Å ⁻²)	9.44
Volfraction	0.01
Fractal_dim	2.9286
Cor_length (Å)	16330
Fitting error χ^2	0.2294

Table S5 SAXS fitting results of MeO-FlavP₁ in aqueous solution (10 g L⁻¹)

Polymer	MeO-FlavP ₁
Model	Fractal core shell
Scale	92.55
Background (cm ⁻¹)	0.04281
Radius (Å)	19.691
Thickness (Å)	29.682
Sld_core (10 ⁻⁶ Å ⁻²)	13.797
Sld_shell (10 ⁻⁶ Å ⁻²)	9.663
Sld_solvent (10 ⁻⁶ Å ⁻²)	9.44
Volfraction	0.01
Fractal_dim	2.7811
Cor_length (Å)	480.57
Fitting error χ^2	0.3108

11. Supplementary TEM images of flavylum-containing polymers

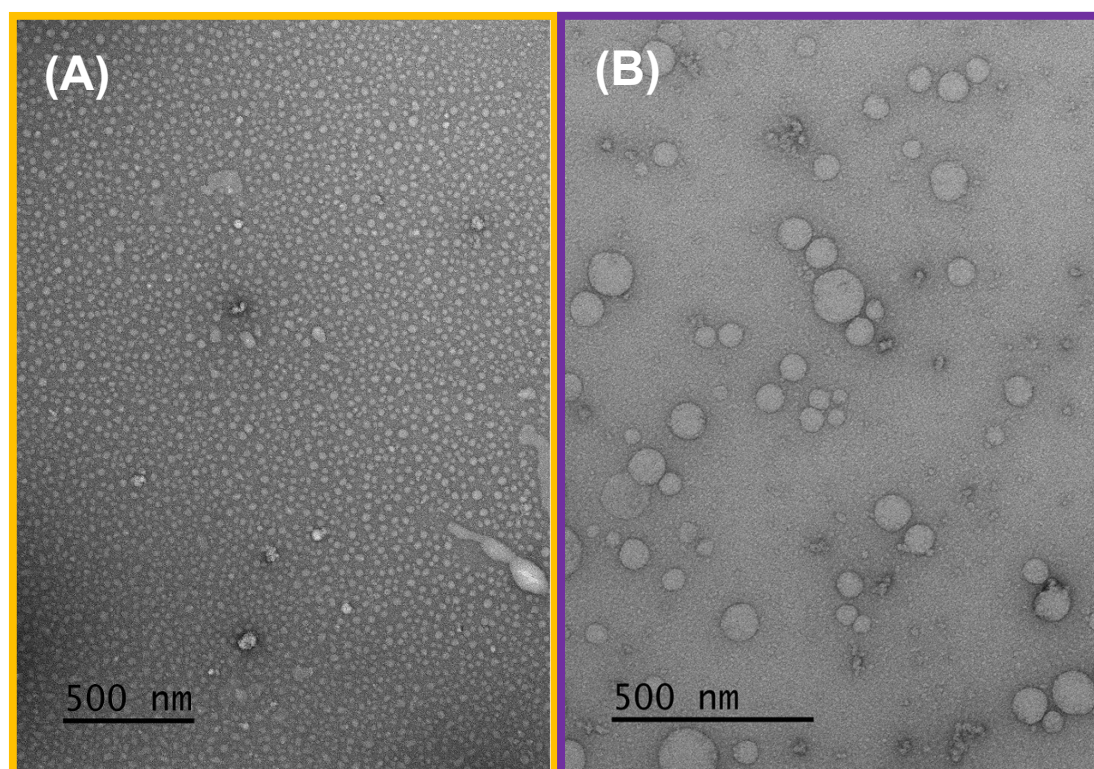


Fig. S16 Conventional TEM micrograph of aggregates formed by drop casting flavylum-containing solutions on the copper grids: (A) MeO-FlavP₁ (aq. 1 g L⁻¹) and (B) Et₂N-FlavP₁ (aq. 1 g L⁻¹), the samples were negatively stained by uranyl acetate (2 wt%).

12. References

- (1) Küster, F.; Thiel, A. *Tabelle per le Analisi Chimiche e Chimico-Fisiche*, 12th edn. ed. Milano: 1982; pp 157-160.
- (2) Kirby, N. M.; Mudie, S. T.; Hawley, A. M.; Cookson, D. J.; Mertens, H. D. T.; Cowieson, N.; Samardzic-Boban, V. A low-background-intensity focusing small-angle X-ray scattering undulator beamline. *J. Appl. Crystallogr.* **2013**, *46* (6), 1670-1680. DOI: doi:10.1107/S002188981302774X.
- (3) Jordão, N.; Gavara, R.; Parola, A. J. Flavylum-Supported Poly(N-isopropylacrylamide): A Class of Multistimuli Responsive Polymer. *Macromolecules* **2013**, *46* (22), 9055-9063. DOI: 10.1021/ma401497q.
- (4) Liu, Y.; McDonald, P. W.; Thang, S. H.; Ritchie, C. Flavylum-Containing Stimuli-Responsive RAFT Polymers: Synthesis and Enhanced Stability. *Macromolecules* **2024**, *57* (7), 3451-3461. DOI: 10.1021/acs.macromol.3c02358.
- (5) Roque, A.; Lodeiro, C.; Pina, F.; Maestri, M.; Dumas, S.; Passaniti, P.; Balzani, V. Multistate/Multifunctional Systems. A Thermodynamic, Kinetic, and Photochemical Investigation of the 4'-Dimethylaminoflavylum Compound. *J. Am. Chem. Soc.* **2003**, *125* (4), 987-994. DOI: 10.1021/ja0287276.